

EFFECTS OF EXCHANGED CATION ON THE MICROPOROSITY OF MONTMORILLONITE

DAVID W. RUTHERFORD,¹ CARY T. CHIOU¹ AND DENNIS D. EBEL²

¹ US Geological Survey, Box 25046, MS 408, Denver Federal Center, Denver, Colorado 80225

² US Geological Survey, 3215 Marine Street, Boulder, Colorado 80303

Abstract—The micropore volumes of 2 montmorillonites (SAz-1 and SWy-1), each exchanged with Ca, Na, K, Cs and tetramethylammonium (TMA) ions, were calculated from the measured vapor adsorption data of N₂ and *neo*-hexane by use of *t*- and α_s -plots. The corresponding surface areas of the exchanged clays were determined from Brunauer–Emmett–Teller (BET) plots of N₂ adsorption data. Micropore volumes and surface areas of the samples increased with the size of exchanged cation: TMA > Cs > K > Ca > Na. The SAz-1 exchanged clays showed generally greater micropore volumes and surface areas than the corresponding SWy-1 clays. The vapor adsorption data and *d*(001) measurements for dry clay samples were used together to evaluate the likely locations and accessibility of clay micropores, especially the relative accessibility of their interlayer spacing. For both source clays exchanged with Na, Ca and K ions, the interlayer spacing appeared to be too small to admit nonpolar gases and the accessible micropores appeared to have dimensions greater than 5.0 Å, the limiting molecular dimension of *neo*-hexane. In these systems, there was a good consistency of micropore volumes detected by N₂ and *neo*-hexane. When the clays were intercalated with relatively large cations (TMA and possibly Cs), the large layer expansion created additional microporosity, which was more readily accessible to small N₂ than to relatively large *neo*-hexane. Hence, the micropore volume as detected by N₂ was greater than that detected by *neo*-hexane. The micropore volumes with pore dimensions greater than 5 Å determined for clays exchanged with Na, Ca and K likely resulted from the pores on particle edges and void created by overlap regions of layers. The increase in micropore volumes with pore dimensions less than 5 Å determined for clays exchanged with TMA and possibly Cs could be caused by opening of the interlayer region by the intercalation of these large cations.

Key Words—Exchanged Cation, Interlayer Accessibility, Microporosity, Montmorillonite, Surface Area.

INTRODUCTION

Interactions of low-polarity vapors with soil colloids and clay minerals are governed to a large extent by the porosities of solids, which are reflected in their calculated BET surface areas using inert gases (Brunauer et al. 1938; Mooney et al. 1952; Brooks 1955; Thomas and Bohor 1968; Aylmore et al. 1970a; Gregg and Sing 1982; Lee et al. 1990; Chiou et al. 1993). The possible sources of porosity of a clay include crevices in the particle surface, staggered layer edges, voids created by the overlapping of stacked layers and interlayer regions, if the layers separations are sufficiently large. This will result in a wide distribution of pore sizes, ranging from micropores (<20 Å) to mesopores (20–500 Å). The available pore sizes of a clay would depend on the intrinsic clay properties (for example, layer charge and exchanged cation), sample preparation and sample degassing condition. The surface area of clay will increase with increasing porosity; however, there are limitations on the application of the BET equation for calculating surface area associated with micropores (Brunauer et al. 1938).

Thomas and Bohor (1968) studied the BET (N₂) surface areas of a series of homoionic Mississippi montmorillonites having different exchangeable cations (Li, Mg, Na, Ca, K, Ba, Rb, NH₄ and Cs) with clay samples degassed at 110–500 °C. The degassing temper-

ature was found to have a relatively minor effect on the surface area, whereas the exchanged cation showed a significant effect on the surface area. In general, the measured surface area increased with increasing cationic radius; the values ranged from 68 m²/g for Li-montmorillonite to 138 m²/g for Cs-montmorillonite on samples degassed at 175 °C. It was suggested by Thomas and Bohor that such a difference reflected a certain degree of N₂ penetration between silicate layers.

In their study of the surface areas of homoionic clays determined by N₂ adsorption, Aylmore et al. (1970a, 1970b) argued that, with the possible exception of Cs-montmorillonite, which displays a greater layer separation, the N₂ penetration between layers of dry montmorillonite clay would be nearly impossible because of the excessive work required to expand closely spaced layers. According to Aylmore and Quirk (1967), the surface area of dry montmorillonite determined by N₂ adsorption was essentially a measure of the area external to “quasi-crystalline overlap” regions and the differences in specific surface area between homoionic montmorillonites were attributed partly to differences in particle size and partly to variations in accessibility of voids caused by quasi-crystalline overlap with size of the exchangeable cations. It was suggested that the quasi-crystalline overlap

regions produce slit-shaped and wedge-shaped pores of various separations (Aylmore and Quirk 1967). For slit-shaped pores, the plate separation may range from 1 layer width (about 9–10 Å) to several layer widths; although not specified, the wedge-shaped pores may have a similar range of dimensions. As a whole, the pore dimensions of quasi-crystalline overlap regions should be relatively large in comparison with the interlayer spacing of most dry exchanged clays (usually <5 Å).

While the differences in surface area between relatively homoionic montmorillonites will reflect the differences in porosity (or microporosity) between the clays, the surface area data do not provide a direct measurement of the clay microporosity. Moreover, the surface areas of micropores having molecular-size dimensions cannot be unequivocally defined and quantified by any gas-adsorption method (such as BET method) because of the pore filling of the adsorbate. The low relative-pressure range at which the vapor (such as N₂) exhibits pore filling is within the range where the vapor adsorption data are used for calculation of BET surface areas. The occurrence of micropore filling may either overestimate or underestimate the actual surfaces, depending on the pore size and its geometry. Because of the problem in defining and measuring surface areas for micropores, the differences in BET surface areas of the exchanged clays are only a relative measure of their micropore volumes. It would therefore be of interest to measure the micropore volumes of the clays and to investigate their dependence on the exchanged cation. Such analysis has not been performed for a series of cation-exchanged montmorillonites, and this information should give useful insight into the likely sources of microporosity in clays.

In this study, we used the measured vapor isotherms of N₂ and *neo*-hexane on 2 source montmorillonite clays (SAz-1 and SWy-1) with different exchanged cations (Na, K, Ca, Cs and TMA) to investigate the effect of cation type on clay microporosity. Isotherms of these vapors on a nonporous kaolinite (KGa-2) were measured as reference standards. Since N₂ and *neo*-hexane have limiting molecular dimension of about 3.5 and 5.0 Å, respectively, a comparison of the micropore volumes calculated from their respective vapor adsorption data facilitates the analysis of the microporosity associated with fine pore structures (that is, the interlayer spacing) whose dimensions fall somewhere between 3.5 Å and 5.0 Å. The combined data of vapor adsorption and measured *d*(001) spacings enhance the evaluation of the accessibility of interlayer spacings to a given vapor. The *d*(001) spacings alone, which show average layer separations, may not be sufficiently illustrative of the extent of their accessibility to vapors if layer separations are not uniform or if vapor adsorption affects the layer spacing. In addition,

intercalation of large cations (large alkylammonium ions) into clay may produce large *d*(001) spacings but limited interlayer voids (micropores) if these ions occupy much of interlayer spacings.

THEORETICAL CONSIDERATION

The BET method for calculating the surface areas (or the apparent surface areas) of solids using nonpolar vapor adsorption data has been described in a number of earlier publications (Brunauer et al. 1938; Gregg and Sing 1982; Chiou et al. 1993). Briefly, the BET plot enables the determination of the statistical monolayer capacity of a reference adsorbate on the solid, which is then used together with the molecular area of the adsorbate to determine the solid's surface area. For relatively nonporous solids, the BET method gives accurate measures of the available surfaces whereas the measured areas for microporous solids are subject to uncertainties because of the occurrence of pore filling in vapor adsorption. Nonetheless, the BET area serves as a useful reference to the porosity of the solid.

Whereas the calculated BET surface areas of relatively homoionic clays reflect the differences in their total porosities (Aylmore and Quirk 1967), more direct analytical methods for the micropore volumes of solids are in order. The *t*-method of de Boer et al. (1966) and the α_s -method of Sing (1969) are commonly used to calculate the micropore volume from vapor adsorption data.

In the *t*-plot of de Boer et al., the adsorbed N₂ volume (*V*) is plotted against the statistical thickness (*t*) of the adsorbed N₂ layer to yield the micropore volumes and nonporous surface areas of solids on the basis that (Remy and Poncelet 1995):

$$V = V_m + 10^{-4} S_0 t \quad [1]$$

where *V* is the total volume of N₂ adsorbed (cm³/g), *V_m* is the volume of N₂ adsorbed in the micropores (cm³/g), *S₀* is the nonporous surface area of the solid (m²/g), *t* is the statistical thickness of the adsorbed N₂ layer (Å), and 10⁻⁴ is a conversion factor. The value of *t* as a function of *P/P⁰* is obtained from the results on a reference solid. A universal *t*-curve of N₂ on nonporous solids has been established (de Boer et al. 1966), which gives:

$$t = [13.99/(0.034 - \log(P/P^0))]^{0.5} \quad [2]$$

where *t* is in Å. If the plot of *V* versus *t* gives a straight line passing through the origin, the test solid is considered to be free of micropores. For a microporous test solid, the *t*-plot shows a straight line at high *t* and a concave-down curve at low *t*; the extrapolation of the upper linear line to *t* = 0 gives a slope of *S₀* and an intercept of *V_m*.

The α_s plot is an alternative version of the *t*-plot. In this method, the amount adsorbed at some fixed *P/P⁰* of a (nonpolar) vapor on a nonporous reference sample

Table 1. Cation exchange analysis of exchanged montmorillonites.

	Exchangeable cations (meq/100 g)					Total
	Ca	Na	K	Cs	TMA	
SAZ-1						
Ca	109	0.07	0.46	0.03	—	110
Na	28.7	83.0	0.43	0.00	—	112
K	2.84	0.07	108	0.00	—	111
Cs	0.72	0.08	0.10	102	—	103
TMA	—	—	—	—	119	119
SWy-1						
Ca	76.8	0.43	0.53	0.02	—	77.8
Na	11.0	52.8	1.94	0.00	—	65.8
K	5.72	2.48	58.0	0.01	—	66.2
Cs	1.46	0.38	0.55	79.8	—	82.1
TMA	—	—	—	—	83.9	83.9

is first normalized to that at $P/P^0 = 0.4$ ($\alpha_s = Q/Q_{0.4}$, where Q is the vapor uptake) to produce a standard α_s -curve rather than a t -curve. The α_s -curve is then used to construct an α_s -plot from the isotherm of the vapor on a test solid, just as the t -curve is used to construct a t -plot. The reference sample is chosen as a nonporous solid having a chemical composition similar to that of the test solid. Similar to t -plot, the α_s -plot gives a straight line passing through the origin if the test solid is free of micropores; for a microporous solid, the α_s -plot shows a straight line at high α_s , and a curve at low α_s , and the extrapolated intercept from the upper linear line gives the micropore volume. If mesoporosity is present in the test sample, there will be an upward deviation from a straight line at relatively high t and α_s .

Unlike the t -plot, the applicability of the α_s -plot is not restricted to the use of N_2 data. This enables separate α_s -plots to be constructed from the respective adsorption data of N_2 and *neo*-hexane on all cation-exchanged clays. The α_s -plot offers a particular advantage in evaluating the microporosity of an exchanged clay as sensed by nonpolar vapors of different molecular sizes. If a molecular sieving occurs for large adsorbates but not for small adsorbates, one would expect to find the microporosity based on the former to be reduced.

To prepare α_s -plots for adsorption of N_2 and *neo*-hexane on exchanged montmorillonites, the standard α_s -curves for these vapors are constructed from their adsorption isotherm on kaolinite. Kaolinite (KGa-2) is considered as a suitable reference solid because of the similarity of its chemical composition to that of montmorillonite and because of its noted absence of measurable microporosity as determined by the t -plot of N_2 adsorption data on kaolinite using the universal t -curve (Equation 2) as reference standard.

EXPERIMENTAL SECTION

Materials

Arizona montmorillonite (SAZ-1), Wyoming montmorillonite (SWy-1) and Georgia kaolinite (KGa-2) were obtained from the Source Clays Repository, the Clay Minerals Society, Department of Geology, University of Missouri, Columbia, Missouri. The clays have nominal cation exchange capacities (CECs) of 120 meq/100 g for SAZ-1, 76 meq/100 g for SWy-1 and 3.3 meq/100 g for KGa-2. Detailed descriptions of these clays are provided by van Olphen and Fripiat (1979). Chemical analysis of the $<0.1 \mu\text{m}$ fraction of the smectites is found in Eberl et al. (1986).

Reagent grade CaCl_2 , NaCl , KCl , CsCl and TMA bromide were used to prepare the relatively homoionic montmorillonite clays. Reagent grade (99% purity) *neo*-hexane and ultrahigh-purity N_2 and He were used in vapor adsorption experiments.

The clay samples were purified by suspending the samples in distilled water and allowing to settle to remove coarse grains and quartz. Relatively homoionic clays were prepared by mixing approximately 3 mol of cation per mol of CEC in distilled water for 24 h. Cations used were Ca, Na, K, Cs and TMA. The suspension was centrifuged, the solution was aspirated off and a fresh solution with cation was added. This procedure was repeated 3 times. The clays were washed by distilled water followed by centrifugation and aspiration until the aspirated solution tested negative with AgNO_3 . The samples were finally freeze-dried.

In addition to the freeze-dried samples, a series of SAZ-1 clays exchanged with Ca, Na, K and TMA cations were similarly prepared, except that they were oven-dried and then ground with a mortar and pestle. The freeze-dried and oven-dried samples showed comparable surface area and porosity characteristics. The BET derived surface areas varied by less than 10% between preparation methods, while total pore volumes were 14–32% higher for oven-dried samples and micropore volumes were 8–27% lower for oven-dried samples. The vapor sorption data presented in this report were obtained from the freeze-dried samples.

Since cation exchange with monovalent cations is not expected to be 100% and the washing steps could be expected to result in some hydrolysis, the samples were analyzed for exchangeable cation and the results are given in Table 1. The freeze-dried clay samples were extracted with 10% (v/v) hot nitric acid for 24 h and analyzed for exchanged Na, K and Ca by inductively coupled plasma (ICP) spectroscopy and for Cs by flame emission spectroscopy. The organic carbon (OC) contents for TMA-exchanged clays were determined by differences between amounts of total C determined by high-temperature combustion and amounts of carbonate C determined by acidification and coulometric analysis.

X-ray Diffraction

The clays were prepared for X-ray diffraction (XRD) by sedimentation on glass slides. The slides were heated at 120 °C for 48 h, stored in a desiccator over CaCl₂ drying compound and X-rayed in an environmental cell containing CaCl₂ drying compound. The samples were scanned in steps of 0.02 °2θ with counting times of 1 min/step, using an automated Siemens D500 XRD system having D5000 software, incident beam soller slits, 1° divergence and receiving slits and a graphite monochromator. The measured $d(001)$ spacings from XRD data did not vary significantly between samples prepared by sedimentation of clay-water slurries on glass plates and by using freeze-dried materials in random orientation mounts. To determine the net 2:1 layer expansion introduced by the cation exchange of both SAz-1 and SWy-1 clays, it is assumed that the dry smectite 2:1 layer has the thickness of a pyrophyllite 2:1 layer, about 9.2 Å.

Vapor Adsorption

The apparatus and procedure used for determination of *neo*-hexane adsorption isotherms has been described previously (Chiou et al. 1993). Briefly, the experiment consisted of equilibrating the vapor and sample in a sorption chamber containing a Cahn electrical microbalance from which a test clay sample hangs in a small glass cup. The clay sample (100 mg) was heated at 100 °C for 24 h inside the chamber and then cooled to room temperature under a vacuum of 10⁻⁶ torr to remove moisture and to set the "dry sample weight". The temperature of the sorption chamber was controlled by laboratory air maintained at 24 ± 1 °C. The liquid *neo*-hexane was purified by vacuum distillation to remove residual air and volatile impurities and then introduced into the sorption chamber for establishment of equilibrium. A change in sample weight resulting from vapor uptake was recorded as an electrical signal from the balance. The equilibrium pressure of the vapor was recorded by a Baratron pressure gauge. Isotherms were constructed by relating the weight of vapor uptake per unit weight of the clay (mg/g) as a function of the relative pressure (P/P°).

The adsorption of N₂ onto clay was determined at liquid N₂ temperature using a Gemini 2360 surface area analyzer (Micromeritics). The test sample was outgassed by heating at 200 °C under a flow of ultra-high-purity of He gas for 24 h. Isotherm data were recorded at P/P° between 0.05 and 0.95.

Surface Areas and Pore Volumes

The apparent surface areas of clay samples were obtained from the statistical monolayer capacities of N₂ from BET plots along with the respective molecular area (a_m) of N₂. An a_m value of 16.2 Å² was assigned for N₂. The micropore volume and the open surface

area of the clay were determined by both t -method and α_s -method using N₂ data and by α_s -method using *neo*-hexane data. The total pore volume of the clay was calculated from the adsorbed N₂ mass at the relative pressure (P/P°) of 0.95 and the use of liquid N₂ density (0.808 g/mL).

Limiting Molecular Dimensions

The limiting molecular dimension of N₂ is taken as 3.54 Å, which is the thickness of a single N₂ molecular layer (de Boer et al. 1966). The limiting molecular dimension of *neo*-hexane (5.04 Å) was determined from the bond angles and van der Waals radii of carbon and hydrogen atoms for the molecular conformation that gives minimum molecular thickness.

RESULTS AND DISCUSSION

Adsorption isotherms of N₂ at liquid N₂ temperature and of *neo*-hexane at room temperature on SAz-1 and SWy-1 montmorillonites substituted with Ca, Na, K, Cs and TMA ions are shown in plots of the vapor uptake (Q) versus the relative pressure (P/P°) in Figures 1–5. The corresponding isotherms on kaolinite (KGa-2) are shown in Figure 6. All vapor isotherms are type-II in shape (Gregg and Sing 1982). In all cases, N₂ shows a higher mass uptake from low to moderate P/P° than *neo*-hexane. This difference results to a large extent from the greater mass per unit area for N₂ than for *neo*-hexane. At P/P° near 1, where a substantial vapor condensation takes place on external surfaces, the 2 vapors show more comparable capacities. In many clay systems, the N₂ isotherms exhibit sharper curvatures than *neo*-hexane isotherms at low P/P° , which suggests that the heat of adsorption per unit area (or per unit volume) is higher for N₂ than for *neo*-hexane.

The total surface areas from BET plots and the open surface areas from t -plots by use of N₂ adsorption data for SAz-1 and SWy-1 clays are given in Table 2. The total pore volumes of the clays as determined from N₂ adsorption at $P/P^\circ = 0.95$ and the related micropore volumes as determined by both t -method and α_s -method using N₂ data are shown in Table 3.

As seen, there are significant micropore volumes associated with both SAz-1 and SWy-1 clays. The micropore volumes determined by the 2 methods are in good agreement, which lends further support to the use of KGa-2 kaolinite as a reference solid in α_s -plot. Based on the average micropore volumes by the 2 methods, the percentage of micropore volumes to total volumes are generally large and comparable for all SAz-1 clays (45–64%); for SWy-1 clays, the values range from 14% for Na clay to 66% for TMA clay. For both SAz-1 and SWy-1 clays, the effect of exchanged cation on micropore volume and total volume follows the order of TMA > Cs > K > Ca ≥ Na. SWy-1 clays exchanged with Ca, Na and K show con-

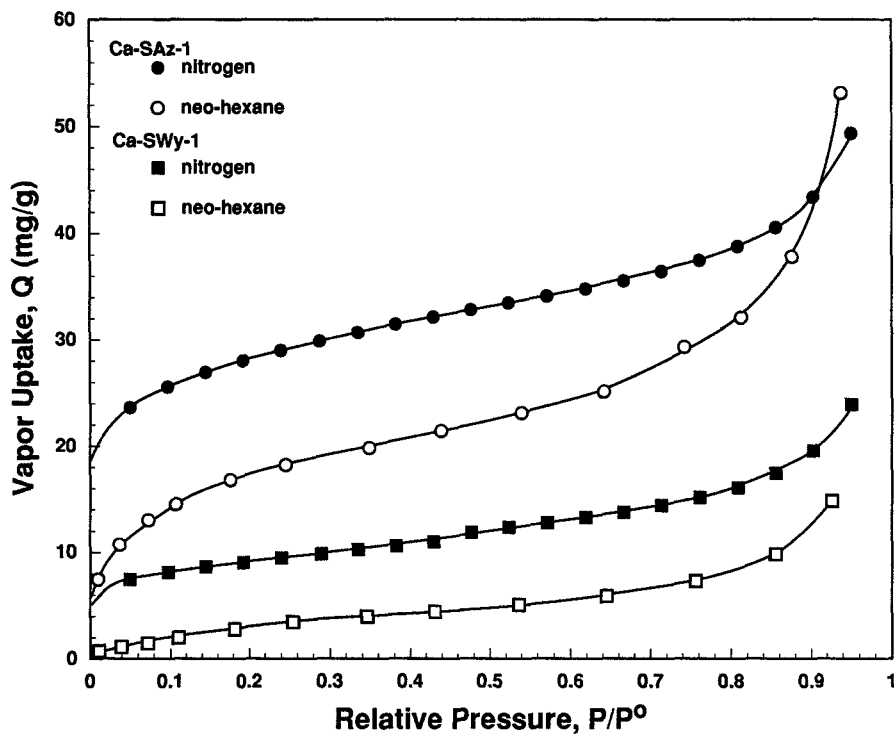


Figure 1. Adsorption of N₂ and *neo*-hexane vapors on Ca-exchanged SAz-1 and SWy-1 clays.

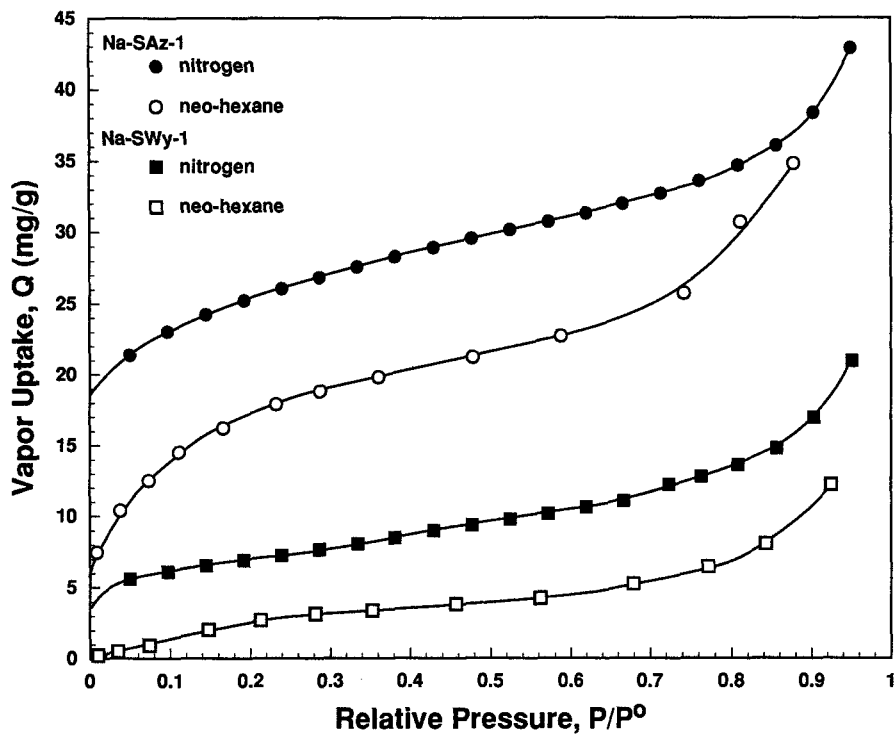


Figure 2. Adsorption of N₂ and *neo*-hexane vapors on Na-exchanged SAz-1 and SWy-1 clays.

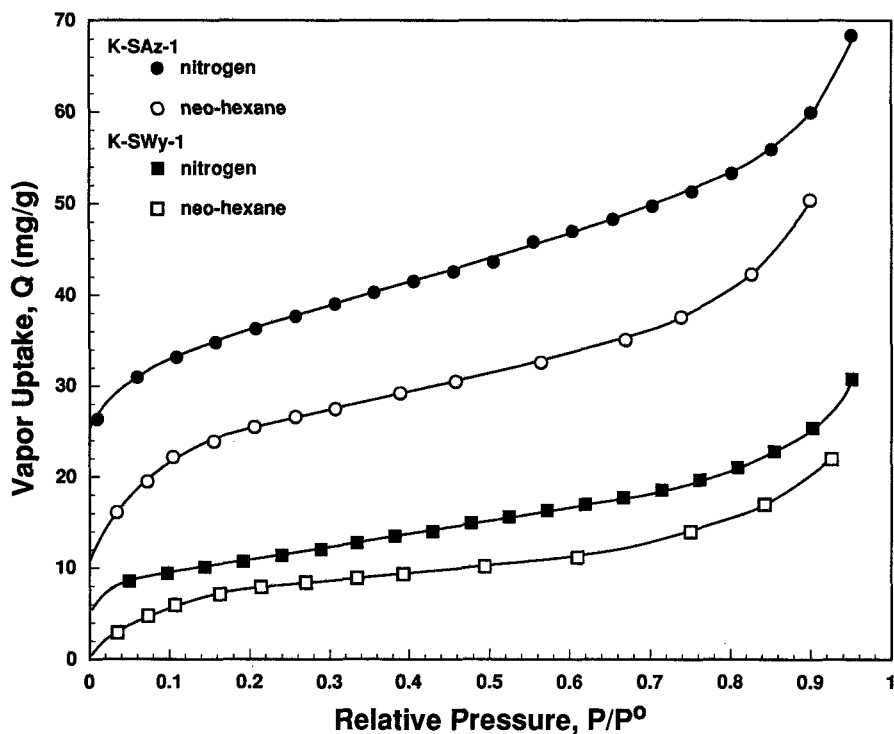


Figure 3. Adsorption of N_2 and *neo*-hexane vapors on K-exchanged SAz-1 and SWy-1 clays.

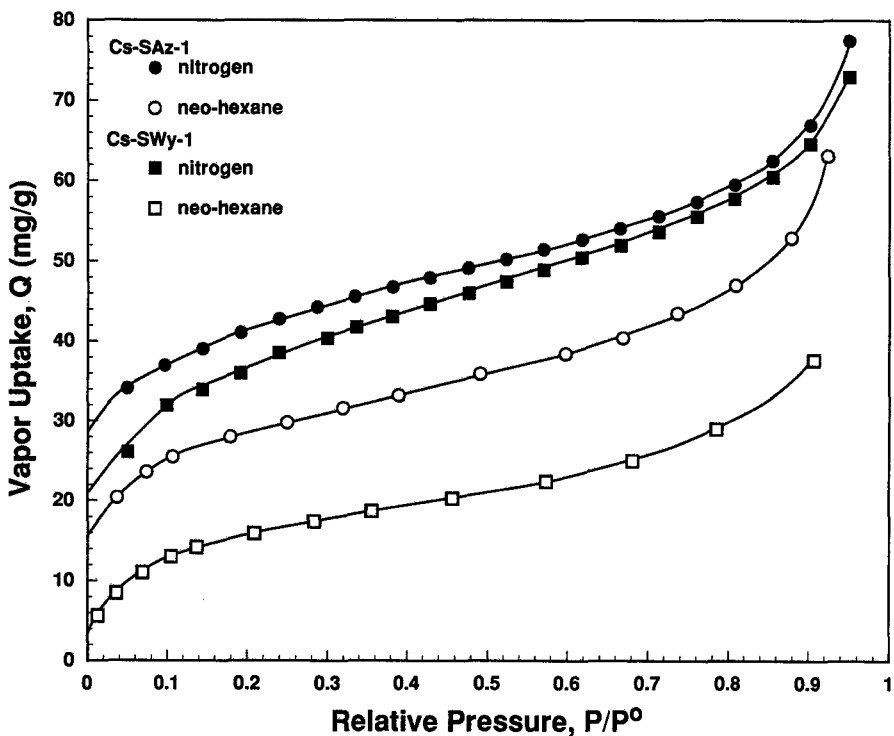


Figure 4. Adsorption of N_2 and *neo*-hexane vapors on Cs-exchanged SAz-1 and SWy-1 clays.

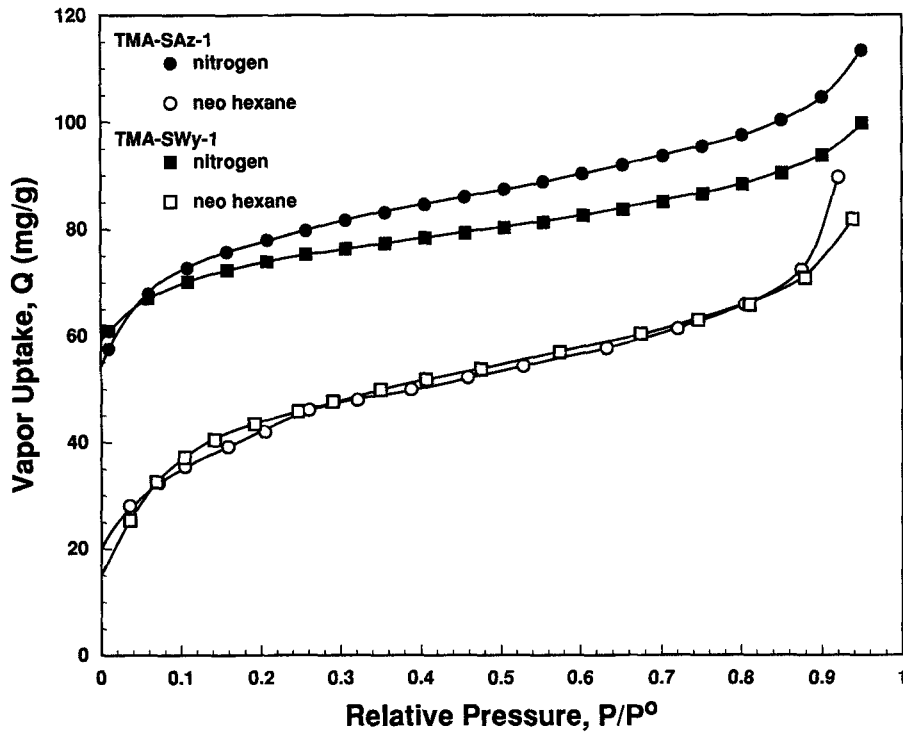


Figure 5. Adsorption of N₂ and neo-hexane vapors on TMA-exchanged SAz-1 and SWy-1 clays.

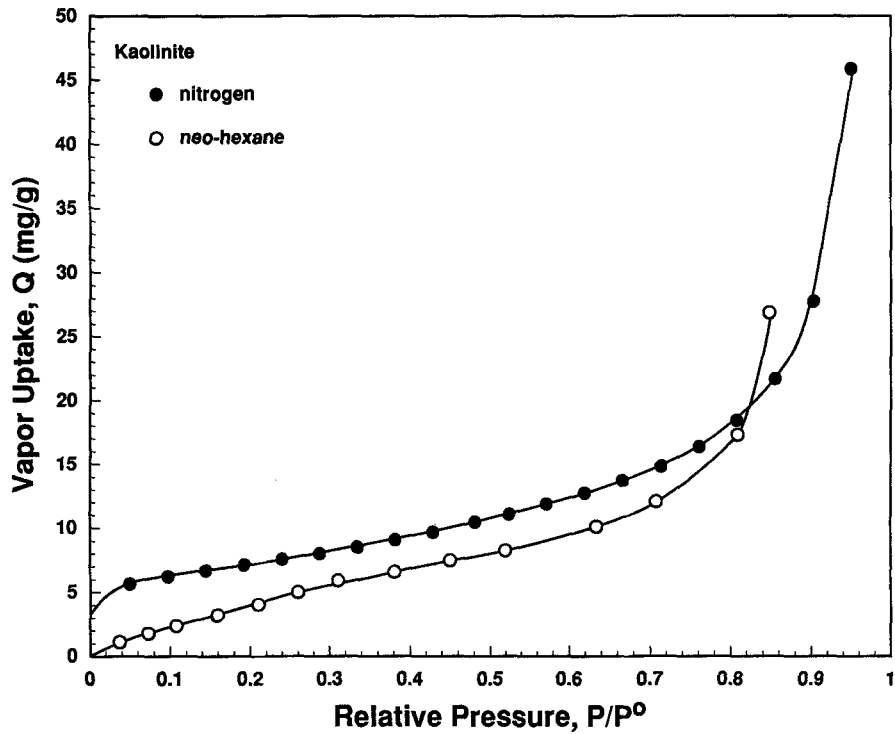


Figure 6. Adsorption of N₂ and neo-hexane vapors on kaolinite (KGa-2).

Table 2. Comparison of total surface area, open surface area, and micropore surface area of exchanged montmorillonites and a reference kaolinite based on N₂ adsorption data.

Clay type	Total surface area by BET (m ² /g)	Open surface area by <i>t</i> -method (m ² /g)	% Surface area contributed by micropores (%)
SAz-1			
Ca	71.5	17.2	76
Na	64.1	14.4	78
K	97.1	26.4	73
Cs	107	29.6	72
TMA	204	29.3	86
SWy-1			
Ca	24.0	12.4	48
Na	18.9	12.5	34
K	29.9	17.6	41
Cs	98.8	30.8	69
TMA	191	24.0	87
KGa-2	21.0	21.1	0

siderably smaller micropore volumes than the rest, while their total pore volumes are comparable with others. The measured micropore volumes of the exchanged clays from either *t*-plot or α_s -plot of the N₂ equal approximately the liquid absorbate volumes at $P/P^0 \leq 0.1$, which is consistent with the strong vapor condensation onto micropore structures. The same is true with the micropore volumes obtained from the adsorption data of *neo*-hexane.

There is a good relationship between total BET surface areas and micropore volumes of the clays, suggesting that a large fraction of the surface area is associated with the micropore. The percentage of micropore area (the difference between the BET surface area and the open surface area derived from the *t*-method) to BET surface area for SAz-1 clays is generally high (72–86%); the values for SWy-1 clays vary from 34% for Na clay to 87% for TMA clay. However, the micropore surface areas of these exchanged clays should be considered as relative rather than absolute measures because of the difficulties previously mentioned in quantifying the surface areas of micropores.

Micropore volumes obtained by α_s -plots of N₂ and *neo*-hexane data with kaolinite as the reference solid are shown in Table 4. A reasonable agreement is found for the values obtained by use of N₂ and *neo*-hexane data for SAz-1 clays exchanged with Ca, Na, K and Cs and for SWy-1 clays with K. A relatively large discrepancy is noted for TMA-SAz-1, Cs-SWy-1 and TMA-SWy-1, in which the N₂ data give higher micropore volumes. While the micropore volumes for Ca- and Na-SWy-1 clays obtained from N₂ data are also much greater than the corresponding values obtained from *neo*-hexane data, the absolute micropore volumes are too small to account quantitatively for the differences.

Table 3. Comparison of total and micropore volumes of exchanged clays determined from N₂ adsorption data by the *t*-method with universal *t*-curve as the reference and by the α_s -method with kaolinite as the reference solid.

Clay type	Total pore volume† (mL/g)	Micropore volume		Average % micropore‡ (%)
		<i>t</i> -method (mL/g)	α_s -method (mL/g)	
SAz-1				
Ca	0.061	0.030	0.026	49
Na	0.053	0.028	0.024	52
K	0.085	0.039	0.033	46
Cs	0.096	0.043	0.040	45
TMA	0.140	0.090	0.082	64
SWy-1				
Ca	0.030	0.007	0.007	23
Na	0.026	0.004	0.004	14
K	0.038	0.008	0.009	20
Cs	0.090	0.039	0.030	43
TMA	0.125	0.084	0.081	66

† Total pore volume is measured at P/P^0 of 0.95 and includes pores with radii up to 200 Å.

‡ Based on the average micropore volumes by *t*-method and α_s -method.

In systems such as SAz-1 clays saturated with Ca, Na and K ions, where the 2 sets of micropore volumes show a reasonable agreement and where the distance between 2:1 layers (≤ 1 Å) are much smaller than the limiting molecular dimensions of N₂ (3.5 Å) and *neo*-hexane (5.0 Å), the majority of accessible micropores are considered to have dimensions more than 5.0 Å, that is, there is no significant population of interlayers (or other fine pores) with separations between 3.5–5.0 Å. Here, the slightly higher micropore volumes as detected by N₂, as compared to those detected by *neo*-hexane, could result partly from a more efficient molecular packing of small N₂ molecule over that of more

Table 4. Micropore volumes of exchanged clays measured by N₂ and *neo*-hexane adsorption data and $d(001)$ values determined by XRD.

Clay type	Micropore volume†		$d(001)$ (dried) (Å)	Interlayer‡ opening (Å)
	N ₂ (mL/g)	<i>neo</i> -hexane (mL/g)		
SAz-1				
Ca	0.026	0.020	9.70	0.50
Na	0.024	0.021	9.75	0.55
K	0.033	0.033	10.0	0.80
Cs	0.040	0.034	10.9	1.70
TMA	0.082	0.056	13.4	4.20
SWy-1				
Ca	0.007	0.002	9.55	0.35
Na	0.004	0.002	9.69	0.49
K	0.009	0.009	9.96	0.76
Cs	0.030	0.018	10.9	1.70
TMA	0.081	0.060	13.8	4.60

† Using the α_s -method with kaolinite as the reference solid.

‡ Determined as the difference between the $d(001)$ and 9.2 Å (for pyrophyllite).

bulky *neo*-hexane in fine micropores (fine wedge-shaped pores). This is in keeping with enhanced curvatures of N_2 isotherms at low P/P^0 . The situation with Cs-SWy-1 and Cs-SAz-1 clays is less clear in that they exhibit practically the same average spacings between 2:1 layers (about 2.0 Å), but Cs-SAz-1 shows relatively comparable micropore volumes based on N_2 (0.040 mL/g) and *neo*-hexane (0.034 mL/g) data, while Cs-SWy-1 exhibits a much lower micropore volume based on *neo*-hexane (0.018 mL/g) than that based on N_2 (0.030 mL/g). It is possible that Cs-SWy-1 has a wider $d(001)$ distribution than Cs-SAz-1 to give the former a greater population of interlayers with spacings between 3.5 Å and 5.0 Å per unit weight, which enables it to more selectively adsorb N_2 over *neo*-hexane. In the case of TMA-SAz-1 and TMA-SWy-1 clays, which show a marked increase in micropore volume, the greater microporosity as detected by N_2 than by *neo*-hexane and related spaces between 2:1 layers (4.2 Å for TMA-SAz-1 and 4.6 Å for TMA-SWy-1) suggest that interlayers are much more accessible to N_2 than to larger *neo*-hexane.

A fundamental difference exists between the properties of SAz-1 clays and SWy-1 clays in that the cation exchange affects the microporosity and surface area for SWy-1 clays to a much greater extent than it does for SAz-1 clays. With the exception of TMA and possibly of Cs-exchanged clays, where the expanded interlayer spacings make a large contribution to microporosity, the relatively high and comparable micropore volumes and surface areas for all SAz-1 clays may be attributed to greater amounts of microporous structures with staggering stacked-layers edges and layer overlap regions per unit weight of the clay. When clay interlayers are intercalated with large cations (such as TMA and possibly Cs), the large layer expansion produces additional microporosity, provided that the expanded interlayer spacings are not substantially filled by the intercalated ions and that the sample preparation does not significantly affect the micropore structures elsewhere. Gast and Mortland (1971) and Clementz and Mortland (1974) found that the dry Wyoming (Upton) montmorillonite exchanged with tetrapropylammonium (TPA) ions produces a greater $d(001)$ spacing (14.6 Å) than the corresponding TMA-clay (13.6 Å) but a considerably lower BET (N_2) surface area (30 m²/g) than the corresponding TMA-clay (220 m²/g), due presumably to the filling of the layer spacings by bigger TPA ions. By the same reasoning, the SAz-1 clay exchanged with tetraethylammonium (TEA) ions produces a greater $d(001)$ (14.2 Å) but a significantly lower surface area (93.0 m²/g) (unpublished results) than the corresponding TMA-SAz-1 clay.

In their comparison of the surface areas of homoionic clays, Aylmore and Quirk (1967) also found the surface areas of Wyoming bentonites exchanged with

Na and Ca to be significantly lower than those of the corresponding Redhill montmorillonites. The lower surface areas for Wyoming bentonites were attributed to their larger lateral dimensions of elemental silicate sheets than those of Redhill montmorillonite. Hence, if the 2 source clays have similar microporous structures at crystal edges or quasi-crystal overlaps, the one with smaller elemental-sheet dimensions would produce higher microporosity and surface area per unit weight. The differences in total surface area between Arizona (SAz-1) and Wyoming (SWy-1) clays exchanged with Na, Ca and K in this study, which are due largely to differences in microporosity, may be related to a similar disparity in the dimensions of their elemental silicate sheets.

SUMMARY

The t -plot by use of de Boer's universal t -curve as the reference and α_s -plot by use of kaolinite (KGa-2) as the reference of N_2 adsorption data give relatively consistent micropore volumes for various cation-saturated montmorillonite clays, which validates the use of kaolinite (KGa-2) as a nonporous reference for montmorillonites. The presence of micropores in both SAz-1 and SWy-1 clays and the strong correlation between micropore volume and measured BET (N_2) surface area show that the difference in surface area of these serial clays is attributable to differences in their microporosity, which is significantly affected by the size of exchangeable cation and the source of the clay. The relatively high microporosity and surface area for the Arizona clay in comparison with that of the Wyoming clay is speculated to result from smaller lateral dimensions of the elemental silicate sheets for the former, which produce more microporosity per unit weight of the clay.

The combined N_2 and *neo*-hexane adsorption data and $d(001)$ spacings manifest that the interlayer spacings of montmorillonites exchanged with small metal cations (such as Na, Ca and K) are usually too small to be even accessible to small nonpolar gases (such as N_2). Cesium montmorillonite represents an intermediate system, where part of the interlayer spacings may be accessible to small N_2 but its accessibility to large nonpolar gases (such as *neo*-hexane) is limited. Intercalation of large TMA ions produces significant amounts of microporosity within silicate layers, which are readily accessible to N_2 , but the accessibility of these micropores to other nonpolar gases would depend on the molecular dimensions of the gases.

REFERENCES

- Aylmore LAG, Quirk JP. 1967. The micropore size distribution of clay mineral systems. *J Soil Sci* 18:1-17.
- Aylmore LAG, Sills ID, Quirk JP. 1970a. Surface area of homoionic illite and montmorillonite clay minerals as measured by the sorption of nitrogen and carbon dioxide. *Clays Clay Miner* 18:91-96.

- Aylmore LAG, Sills ID, Quirk JP. 1970b. Reply to comment of Thomas, Bohor and Frost on "The surface area of homioic illite and montmorillonite clay minerals as measured by the sorption of nitrogen and carbon dioxide". *Clays Clay Miner* 18:407–409.
- Brook CS. 1955. Nitrogen adsorption experiments on several clay minerals. *Soil Sci* 79:331–347.
- Brunauer S, Emmett PH, Teller E. 1938. Adsorption of gases in multimolecular layers. *J Am Chem Soc* 60:309–319.
- Chiou CT, Rutherford DW, Manes M. 1993. Sorption of N₂ and EGME vapors on some soils, clays, and mineral oxides and determination of sample surface areas by use of sorption data. *Environ Sci Technol* 27:1587–1594.
- Clementz DM, Mortland MM. 1974. Properties of reduced charge montmorillonite: Tetra-alkylammonium ion exchange forms. *Clays Clay Miner* 22:223–229.
- de Boer JH, Lippens BC, Linsen BG, Broekhoff JCP, van den Heuvel A, Osinga Th J. 1966. The *t*-curve of multilayer N₂-adsorption. *J Colloid Interface Sci* 21:405–414.
- Eberl DD, Šrodoň J, Northrop HR. 1986. Potassium fixation in smectites by wetting and drying. In: Davis JA, Hayes KE, editors. *Geochemical processes at mineral surfaces*, ACS Symp Series 323. Washington, DC: Am Chem Soc. p 296–326.
- Gast RG, Mortland MM. 1971. Self-diffusion of alkylammonium ions in montmorillonite. *J Colloid Interface Sci* 37:80–92.
- Gregg SJ, Sing KSW. 1982. *Adsorption, surface area and porosity*, 2nd ed. London: Academic Pr. p 61–84.
- Lee J-F, Mortland MM, Chiou CT, Kile DE, Boyd SA. 1990. Adsorption of benzene, toluene, and xylene by two tetramethylammonium-smectites having different charge densities. *Clays Clay Miner* 38:113–120.
- Mooney RW, Keenan AG, Wood LA. 1952. Adsorption of water vapor by montmorillonite. I. Heat of desorption and application of BET theory. *J Am Chem Soc* 74:1367–1371.
- van Olphen H, Fripiat JJ. 1979. *Data handbook for clay materials and other non-metallic minerals*. New York: Pergamon Pr. p 16–25.
- Remy MJ, Poncelet G. 1995. A new approach to the determination of the external surface and micropore volume of zeolites from the nitrogen adsorption isotherm at 77 K. *J Phys Chem* 99:773–779.
- Sing KSW. 1969. Surface area determination. In: Everett DH, Ottewill RH, editors. *Proc Int. Symp*; 1970. London: Butterworths. p 25.
- Thomas J Jr, Bohor BF. 1968. Surface area of montmorillonite from the dynamic sorption of nitrogen and carbon dioxide. *Clays Clay Miner* 16:83–91.

(Received 4 March 1996; accepted 15 September 1996; Ms. 2749)